P-ISSN: 2304-3075; E-ISSN: 2305-4360
International Journal of Veterinary Science
www.ijvets.com; editor@ijvets.com
Research Article
DOI: 10.37422/IJVS/20.017

MRI Features of Fetlock and Pastern Regions in 30 Chronically, Un-Treated Lame Draft Horses Confirmed by Postmortem Examination

Yahya M Elemmawy[1*], Ashraf M Abu-Seida[1], Nasser A Senna[1] and Ahmed F Yousef[2]

[1]Department of Surgery, Anesthesiology and Radiology, Faculty of Veterinary Medicine, Cairo University, PO: 12211, Giza, Egypt; [2]Department of Radiology, Faculty of Medicine, Benha University, Benha, Qalyubia, Egypt
***Corresponding author:**

Article History: 20-015 Received: January 15, 2020 Revised: February 20, 2020 Accepted: February 29, 2020

ABSTRACT

Lameness from fetlock and pastern regions is a big challenge to most equine practitioners and produces a detrimental effect on horses' activity and on owners' finances. Nuclear scintigraphy, radiography and ultrasonography are not conclusive when assessing of fetlock and pastern lameness. This study describes the magnetic resonance imaging (MRI) features in 30 draft horses with chronic, un-treated lameness attributable to fetlock and pastern regions as well as confirms these features by postmortem examination. Thirty-three cadaver limbs were collected after euthanasia, imaged by MR and lastly examined grossly. Seventeen lesions were recorded and described using MRI. MRI revealed injuries of both soft and osseous tissues in 24 horses (80%), soft tissue injuries in five horses (16.7%) and bone and cartilage injuries in one horse (3.3%). All horses had multiple MRI abnormalities. The most frequent MR lesions were digital tenosynovitis (n=13), straight sesamoidean desmitis (n=10), osteosclerosis in the distal part of third metacarpal bone (MCIII) or first phalanx (PI, n=10), adhesions between straight sesamoidean ligament (SSL) and deep digital flexor tendon (DDFT, n=9), oblique sesamoidean desmitis (n=7), cartilage erosions of fetlock or pastern joints (n=7), adhesions between proximal digital annular ligament and DDFT (n=6), DDFTendinitis at pre-navicular part (n=6), proximal digital annular desmitis (n=5), subchondral bone cyst of PI (n=3), and cyst like lesions in PI and PII (n=2). In conclusion, MRI played a pivotal role in comprehensive evaluation of fetlock and pastern regions and it is highly recommended for examination of all structures of fetlock and/or pastern regions in chronically lame draft horses.

Key words: Desmitis, Diagnostic imaging, Digital tenosynovitis, Metacarpo-phalangeal joint, Osteosclerosis, Tendinitis

INTRODUCTION

Lameness evaluation in draft horses represents a specific challenge due to the delayed onset of obvious signs of lameness as they are rarely exercised at speeds greater than a trot (Hawkins, 2011).

The fetlock joint is overwhelmed with multiple problems that contribute to most prevalent causes of lameness in all horse disciplines (Pool and Meagher, 1990, Johnston and Nickels, 2011). Commonly, cumulative stress-related bone injury involving bone and/or cartilage and osteoarthritis were recorded. Bone bruise, a significant cause of fetlock and pastern pain, has become well-recognized in horses (Martinelli *et al.,* 1996, Dyson and Murray, 2006).

Proximal sesamoids and components of associated suspensory apparatus are subject to tremendous tensile forces and hyperextension actions and complicate the anatomical structures of the fetlock and pastern regions (Dyson and Murray, 2007).

Most equine practitioners are not well familiarized with the convoluted anatomy of pastern region, so soft tissue injuries are likely underdiagnosed (Johnston and Nickels, 2011). Injury of collateral ligaments, the distal sesamoidean ligaments, and flexor tendons is frequently involved and may produce joint instability and development of ringbone several months later (Smith *et al.*, 2008 and Johnston and Nickels, 2011). Pulling and twisting of the pastern region during draft work beside large body size increase the risk of osteoarthritis of proximal interphalangeal joint (pastern) in draft horses (Knox and Watkins, 2006 and Olive *et al.*, 2009).

Most imaging modalities have several restrictions in fetlock and pastern regions. In many clinical cases, radiography and even scintigraphy can't detect early cartilage loss and subchondral bone injury (Sherlock *et al*, 2009 and Gonzalez *et al.,* 2010). Ultrasonographic evaluation is less sensitive than MRI for several injuries of fetlock and pastern regions such as injuries of the straight and oblique distal sesamoidean ligaments

Cite This Article as: Elemmawy YM, Abu-Seida AM, Senna NA and Yousef AF, 2020. MRI Features of fetlock and pastern regions in 30 chronically, un-treated lame draft horses confirmed by Postmortem examination. Int J Vet Sci, x(x): xxxx. www.ijvets.com

(Sampson *et al.,* 2007). Therefore, MRI had become widely used in fetlock and pastern regions of horses to describe abnormalities of the oblique and straight sesamoidean ligaments, subchondral bone injury, osteoarthritis, cartilage injury, osteochondral fragmentation and proximal sesamoid bone injury (Sampson *et al.,* 2007, Sherlock *et al.,* 2009 and Gonzalez *et al.,* 2010). Moreover, traumas to cancellous bone within the metaphyses and epiphyses were difficultly evaluated in mature horses before advent of MRI (Dyson and Murray, 2006).

This study describes the specific MRI abnormalities encountered in 30 draft horses with advanced degrees of lameness originated from both fetlock and pastern regions and confirms these findings by gross postmortem examination.

MATERIALS AND METHODS

Thirty light draft horses were admitted to Brooke charity hospital, Egypt with lameness originating from fetlock and pastern regions. The examined horses included 21 stallions and 9 mares. The age of these animals ranged from 4 to 12 years and their weight ranged from 350-400 kg. The duration of lameness ranged from 6 to 24 months. Thorough clinical examination and high palmar/plantar perineural analgesia for confirmation of the origin of lameness were carried out. Lameness grades were scaled from 0–5 following AAEP guidelines (AAEP, 2019). Radiographic and ultrasonographic evaluations of fetlock and pastern regions had been performed to guide us to the suspected injured structures before MRI. Due to various reasons other than this study (such as non-tolerated temperament of the horse and severe lameness), all horses were euthanized by I/V administration of an overdose of barbiturates according to AAEP guidelines (AAEP, 2019).

Both affected and contralateral limbs were collected just after euthanasia from the carpal or tarsal level up to the hoof. These limbs were imaged by MR within 8 hours post dissection (Smith *et al.,* 2008).

MRI was performed with the limbs positioned in a 0.3T magnet (Siemens AG 2009, Syngo MR A35, ID: 008, Germany). All images were obtained with a human brain circular coil (Tx Coil) wrapped around the center of the fetlock joint and secured with Velcro straps; the coil extended from a level 5-8 cm proximal to the midpoint of fetlock joint (cover the distal third of McIII/MtIII) to the level of coronary band distally. The contralateral fetlock and pastern regions were examined for comparison in all cases.

To minimize the time of imaging, routine work usually started in all examined horses (N=30) by T1 SE, PD, TIRM and T2 TSE sequences in both sagittal and transverse planes with a slice thickness of 3-5 mm. According to the findings, further sequences were used as shown in (Table 1). Collected images were studied using RadiAnt Digital Imaging and Communications in Medicine (DICOM) Viewer software (Version: 4.6.8.18460) after withdrawing from picture archiving and communication system (PACS). The MRI abnormalities were compared with the findings of Postmortem examination.

Statistical analysis was performed in all recorded co-existing lesions using Pearson Correlation (r). IBM (IBM, NY, USA) SPSS Statistic Version 20 for Windows was applied for statistical analysis. Correlation was significant at the 0.05 level and retested at 0.01 levels (2-tailed).

RESULTS

Thirty-three limbs were affected in the examined horses (n=30). Eighteen horses had a forelimb lameness (10 left forelimbs, five right forelimbs and three both forelimbs) and 12 horses had a hindlimb lameness (five left hindlimb and seven right hindlimb). The degree of lameness ranged from 2/5 to 4/5. With diagnostic analgesia, the lameness resolved completely in 26 horses and not improved significantly in four horses before euthanasia.

None of the examined horses was free from MRI abnormalities involving at least two lesions. MRI of the fetlock and pastern regions revealed injuries of both soft and osseous tissues in 24 horses (80%), soft tissue injuries in five horses (16.7%) and bone and cartilage injuries in one horse (3.3%).

Seventeen MR lesions were recorded including 10 anatomical structures as shown in Table (2). The correlations between the recorded lesions are shown in supplementary (1).

Distal sesamoidean desmitis was reported in 32 limbs including SSL desmitis (n=10), adhesion between SSL and DDFT (n=9), oblique sesamoidean desmitis (n=7), and adhesions between DDFT and proximal digital annular ligament (n=6). The main MR signal characteristic of distal sesamoidean desmitis was generalized hyperintensity in PD, T2, and TIRM images in comparison with contralateral normal limb. T2 TSE and TIRM sequences were critical for definitive diagnosis to exclude magic angle effect.

In 6 cases, the proximo-distal length of hyperintense SSL varied from proximal third (2 horses) to the whole length of SSL (4 horses) with enlargement of cross-sectional area (Fig. 1A&B).

Lesions in the oblique distal sesamoidean ligaments were involved the proximal two thirds of the ligaments or the whole length till the insertion to the proximal phalanx (Figs. 1B-D). Marked enlargement of the cross-sectional area associated with increased signal intensity was observed. The recorded MRI lesions were confirmed by Postmortem findings (Fig. 1D&E).

Digital tenosynovitis was recorded in 13 horses. This lesion was not present solely in the affected horses but it was associated with other injuries like chronic DDFT injuries, distal seasmoidean desmitis or joint problems. In 10 cases, the tendon sheath was partially distended with high signal intensity effusion in all sequences at the level of the PI and PII (Fig. 2A).While in the other 3 cases, the tendon sheath appeared distended along its whole length with high signal intensity effusion from above proximal sesamoid bones and distally to its distal recess just above the navicular bone (Fig. 2B-D).

Table 1: Parameters of MRI pulse sequences used for imaging of fetlock and pastern regions in the examined horses

Sequence	TR (ms)	TE (ms)	FA°	NEX	Matrix size	Slice width (mm)	Gap (mm)	Time
T1 SE	429	11	80	3	250*300	4	4.4	3:42
FLASH 3D	50	17	15	2	222*222	2	2	6:20
T1 3D GE	80	43	180	1	187*230	2	2	4:14
T1 TSE Dixon	1280	34	90	1	300*300	3	4.5	3:15
T2 TIRM	7780	22	180	1	250*250	3	3.3	5:42
T2 TSE	4650	106	180	2	250*250	5	6.5	5:23
T2 FSE	7660	89	180	2	210*210	8	11	3:19
PD	3330	17	180	2	244*244	3.5	4.5	5:39

TR: time of repetition, TE: time of echo, FA: flip angle, SE: spin echo, FLASH: fast low angle shot, GE: gradient echo, TIRM: turbo inversion recovery magnitude, TSE: turbo spin echo, FSE: fast spin echo, PD: proton density.

Table 2: Number, percentage, most useful MRI sequences and imaging planes of the recorded MRI lesions at fetlock and pastern regions of the examined horses

No	Fetlock and pastern lesions	Incidence & %	Sequences	Planes
1	Digital tenosynovitis	13 (43.3%)	T1-weighted &PD	Transverse, sagittal
2	SSL desmitis	10 (33.3%)	T2-TSE &TIRM	Transverse, sagittal
3	Osteosclerosis in distal MCIII	10 (33.3%)	T1 &T2-weighted	Transverse, sagittal, Dorsal
4	Adhesions between SSL and DDFT	9 (30%)	T1 &T2-weighted	Transverse, sagittal, Dorsal
5	Oblique sesamoidean desmitis	7 (23.3%)	T2-TSE &TIRM	Transverse, sagittal
6	Cartilage erosions of fetlock and/or pastern	7 (23.3%)	T2 TIRM, FLASH, PD & TIRM	Transverse, sagittal, Dorsal
7	Adhesions between proximal digital annular ligament and DDFT	6 (20%)	T1 &T2-weighted	Transverse, sagittal, Dorsal
8	DDFTendinitis (Prenavicular part)	6 (20%)	T1-weighted &TIRM	Transverse, sagittal
9	Proximal digital annular desmitis	5 (16.7%)	T1 SE &T2 FSE	Transverse, sagittal
10	Bone exostosis over pastern	5 (16.7%)	T1 GE	Transverse, sagittal
11	Superficial digital flexor tendon disruption	3 (10%)	T1-weighted	Transverse, sagittal
12	Subchondral bone cyst of PI	3 (10%)	T1 &T2-weighted	Transverse, sagittal, Dorsal
13	Cyst like lesion in PI and PII	2 (6.6%)	T1 3D GE, T2 TSE, PD	Transverse, sagittal, Dorsal
14	Collateral desmitis of fetlock joint	2 (6.6%)	T1-weighted &TIRM	Sagittal, Dorsal
15	Common digital extensor tendon disruption	2 (6.6%)	T1 SE &T2 FSE	Transverse, sagittal
16	Extensor branch desmitis of SL	1 (3.3%)	T1-weighted &TIRM	Sagittal, Dorsal
17	Dorsal osteochondral fragmentation (chip fracture) of distal PI	1 (3.3%)	T1 SE	Transverse, sagittal, Dorsal

SSL: straight sesamoidean ligament, DDFT: deep digital flexor tendon, SL: suspensory ligament.

Osteosclerotic lesions of distal MCIII were identified in 10 horses. This abnormality was present on the lateral aspect of the bone in three horses (Fig. 3A&B) and from lateral side of the bone to the medial in one horse (Fig. 3C&D). This lesion appeared as scattered focal signal decrease throughout the trabecular tissue (enostosis like lesion) with trabecular thickening in T1-weighted, PD, and T2 images.

Cartilage injuries were observed by MRI in 7 horses. The cartilage injuries included fetlock erosion (n=4) and pastern erosions (n=3). Compared with the normal contralateral joint (Fig. 4A), the injuries were identified by focal accumulations of hyperintense joint fluid within the cartilage defects on FLASH, PD, DIXON, TIRM and T2 weighted parasagittal images (Fig. 4B&C). The articular lesions were confirmed grossly (Fig. 4D). Cartilage defects were also identified on dorsal aspect of pastern joint (Fig. 5A&B). The lesions were confirmed by Postmortem examination (Fig. 5C).

Collateral sesamoidean desmitis was identified in six horses. The lesion was characterized by thickening of the ligament relative to the contralateral limb and hyperintensity in FLASH, T1 TSE, T2 and PD images in the affected part of the ligament. In one horse with desmitis of the deep part of the lateral collateral ligament, medullary sclerosis of PII was present at the origin of the ligament. Collateral sesamoidean desmitis was found concomitant with DDFT injury, distal sesamoidean desmitis, pastern subluxation, chronic CDET injury (Fig. 6).

Deep digital flexor tendon injury at the level of the PI was reported in six horses. The lesion was characterized by the presence of focal areas of signal hyperintensity dispersed throughout the deep digital flexor tendon, distinct hyperintense core lesions, prominent thickening of the affected lobe and a longitudinal, parasagittal and incomplete split of the lateral border of the tendon (Fig. 6). Hyperintensities and changed contour of DDFT were more obvious in FLASH and T1 3D GE images than in STIR and T2-weighted images. The affected horses experienced adhesions of DDFT with SDFT or distal sesamoidean ligaments.

Proximal digital annular desmitis was seen in 5 horses. The affected animals showed adhesions between the proximal digital annular ligament and dorsal aspect of DFTS, SDFT or DDFT. These adhesions ranged from recent fibrosis with increased signal intensity of inflammatory fluid (Fig. 7A) to old fibrosis of low signal intensity (Figs. 7B). The lesions were confirmed by Postmortem examination (Fig. 7C). The lesion appeared clearly on T1 SE and T2 FSE sequences on transverse and sagittal slices.

In 3 horses, subchondral bone erosions (focal trabecular bone damage or osseous cyst-like lesions, OCLLs) were visible as focal signal hyperintensity surrounded by an area of signal hypointensity. The lesions were usually adjacent to the articular surface. The transverse and sagittal T1 3D GE and T2 TSE images were most useful for recognizing sclerosis-related signal

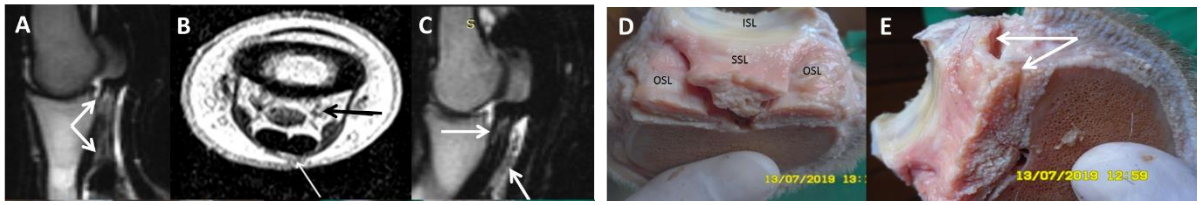

Fig. 1: (A) T2 TSE sagittal image of fetlock in a 12-year-old stallion showing generalized increased intermediate signal intensity involving the whole SSL length (white arrows) till middle scutum (compare with DDFT signal intensity). (B) T1 SE transverse image of fetlock region in a 9-year-old stallion showing higher signal intensity of SSL, extensive disruption of OSL of increased intermediate signal intensity (black arrow) and disrupted sagittal part of SDFT (white arrow) with higher signal intensity of s/c edema. (C) Sagittal T2 TSE image of fetlock joint in a 6 year-old horse showing increased intermediate signal intensity at proximal third of OSL with increased thickness compared with the thickness of DDFT and palmar adhesions to DDFT (white arrows). (D) Postmortem of the horse in figure C showing congested thickened distal sesamoidean ligaments. (E) Abaxial view of figure D showing longitudinal tear (white arrows) in OSL corresponding with MRI in figure C.

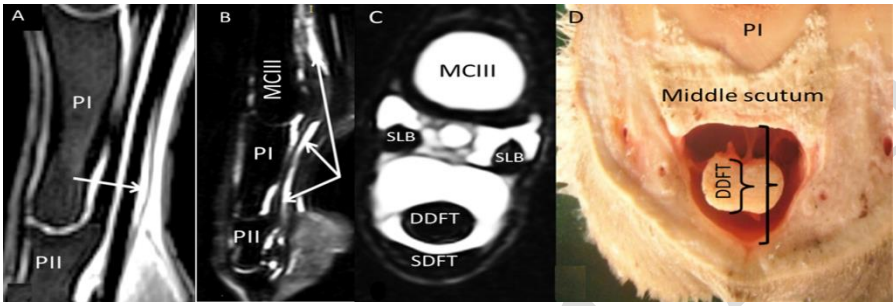

Fig. 2: (A) Sagittal T1 Dixon image of pastern region in a 7 year-old draft mare showing localized DFTenovaginitis at level of distal PI (white arrow). (B) Sagittal T2 TIRM image of phalangeal region in a 9 year-old draft stallion showing generalized digital tenosynovitis (white arrows). (C) T1 SE transverse image of fetlock region in a 7-year-old stallion showing massive effusion of DFTS at the level of suspensory ligament branch (SLB). (D) Postmortem specimen of fetlock region in a 12-year-old draft horse showing massive digital tenosynovitis at the level of middle scutum. PI: first phalanx, PII: second phalanx, MCIII: third metacarpal bone, SDFT: superficial digital flexor tendon, DDFT: deep digital flexor tendon.

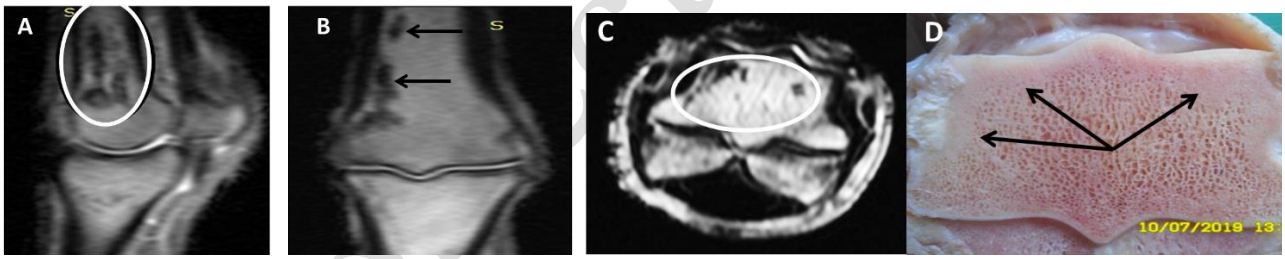

Fig. 3: Sagittal (A) and dorsal (B)T1 3D GE images of MCIII in an 8-year-old draft stallion with osteosclerosis showing areas of low signal intensity (circle& balck arrows) consistent to dense compact bone close to cortical bone and spreading into spongy trabecular bone. (C) Transverse FLASH 3D image of fetlock joint in an 11- year-old draft mare showing areas of low signal intensity consistent to osteosclerosis laterally and medially close to cancellous bone (circle). (D) Postmortem specimen of MCIII in figure C confirming the MRI findings.

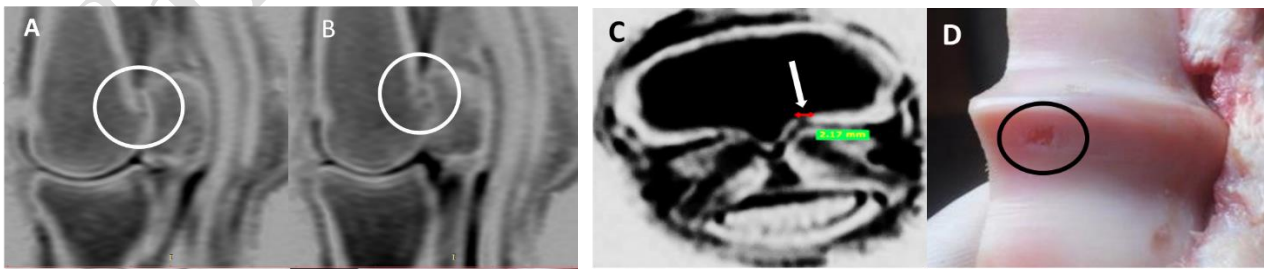

Fig. 4: (A) Sagittal FLASH negative image of fetlock joint in a 12-year-old draft stallion showing normal cartilage of the healthy medial side of the sagittal ridge (circle). (B) Negative sagittal FLASH image of fetlock joint in the same horse in figure A showing cartilage erosion at lateral side of sagittal ridge of distal MCIII (circle). (C) Transverse FLASH image of fetlock joint in a 12-year-old draft stallion showing cartilage erosion (2.17 mm) at the lateral side of sagittal ridge of distal MCIII (white arrow). (D) Postmortem specimen of the same lesion in figure B confirming the MRI findings.

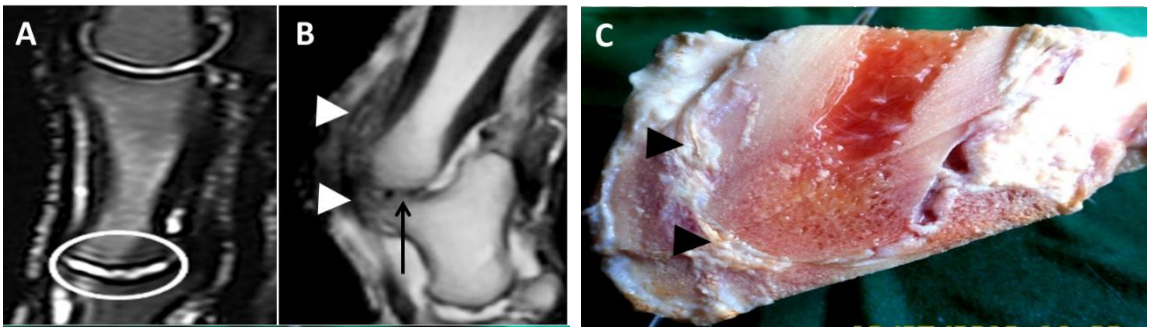

Fig. 5: (A) Sagittal T1 3D GE image of pastern joint in an 8-year-old draft stallion showing spot of entrapped erosion of intermediate signal intensity in cartilage of articular surfaces of distal PI and proximal PII (circle). (B) Sagittal T1 SE image of pastern joint a 9-year-old draft mare with subluxation showing complete loss of subchondral bone of distal PI and extreme thinning of proximal PII subchondral bone, fusion of spongy trabecular bone of distal PI and corresponding of PII (black arrow) and newly osseous tissue at dorsal aspect of pastern joint entrapping CDET (white arrow heads). (C) Postmortem specimen of the same lesion in figure B confirming all MRI findings.

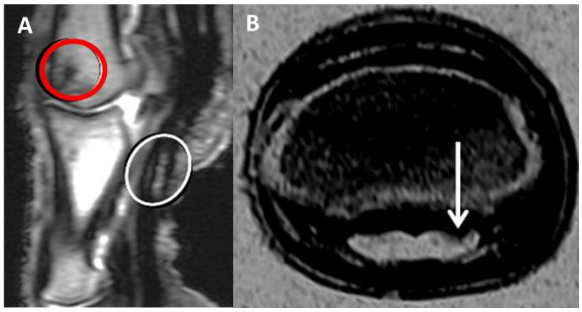

Fig. 6. (A) Sagittal T1 3D GE image of fetlock joint in a 9-year-old draft mare showing increased intermediate signal intensity within DDFT at the level of proximal third of PI with associated abnormal signal at palmar aspect of DDFT corresponding to associated adhesions with SDFT (white circle). Notice the associated osteosclerosis of distal MCIII (red circle). (B) Negative transverse T1 SE image of pastern region in a 7-year-old draft stallion showing dorsal incomplete tear of lateral lobe of DDFT at the level of middle PII (white arrow).

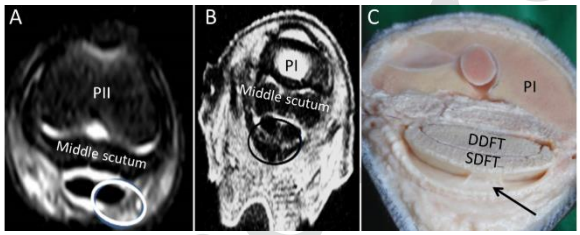

Fig. 7: (A) Transverse T2 2D GE image of pastern region in a 6-year-old stallion showing thickened proximal digital annular ligament and recent fibrosis with increased intermediate signal intensity between PDAL and DDFT (white circle). Notice the associated moderate DFTenosynovitis at the level of middle scutum. (B) T1 SE transverse image of pastern region in an 11-year-old mare showing thickened PDAL and old fibrosis of low signal intensity between PDAL and DDFT at level of middle scutum (black circle). (C) Postmortem specimen of fetlock region in a 9-year-old draft stallion showing thickened PDAL with adhesion to SDFT dorsally at level of fetlock joint (black arrow). PI: first phalanx, PII: second phalanx.

changes (Fig. 8A-C). The PD-weighted images provided good anatomic details of bone including trabecular thickness and density. Occasional obvious normal cystic lesion of PI marrow at the level of thickest part of cortices was reported in a 6-year-old horse (Fig. 8D&E).

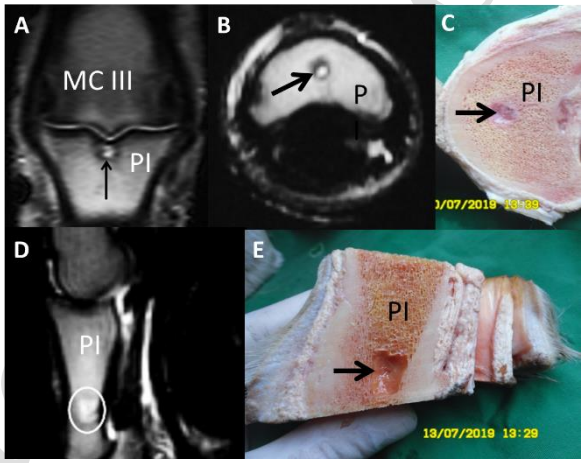

Fig. 8: Dorsal (A) and transverse (B) T1 3D GE images of fetlock joint in a 7-year-old draft mare showing high signal intensity cystic lesion attached to proximal subchondral bone of PI at the level of sagittal groove (black arrows). (C) Postmortem specimen of the same horse in figures A&B confirming the MRI findings (black arrow). (D) Sagittal T2 TSE image of fetlock region in a10-year-old draft mare showing occasional normal finding of high signal intensity cystic like lesion in middle third of PI marrow cavity (white circle). (E) Postmortem specimen of the same horse in figure D showing the same cystic lesion (black arrow) confirming the MRI findings. PI: first phalanx, PII: second phalanx, MCIII: third metacarpal bone.

The most suitable MRI sequences and planes (Magnetom C, Siemens AG 2009, Syngo MR A35, ID: 008, Germany) for each of the previous lesions were collected in Table (2).

DISCUSSION

Diagnosis of lameness originated from fetlock and pastern regions is a big challenge in equine practice. Recently, MRI was introduced in veterinary practice for complete evaluation of both soft and bony tissues of the animal's body. The aims of the present study were to describe MRI features of fetlock and pastern regions in chronically, un-treated lame draft horses and to determine the most useful sequences and planes for the common lesions of these regions. In this study, 80% of the lame horses suffered from lesions originated from both soft and bony tissues of fetlock and pastern regions.

Digital flexor tenosynovitis was the most commonly recorded lesion in the examined horses due to the nature of their work. Moreover, this lesion was usually found as a secondary lesion. Proximal digital annular desmitis, DDFT injuries and SSL desmitis were the associated lesions. In this regard, Smith and Wright (2006) and Arensburg *et al.* (2011) recorded that 78% and 58% of the horses subjected to tenoscopy of DFTS suffered from DDFT longitudinal tear. Gibson *et al.* (1997) added SDFTendonitis to the associated lesions. This could be attributed to spreading of inflammatory reaction to the nearby tissues as mentioned before (Schramme and Smith, 2011). In contrast to Gibson *et al.* (1997), this study revealed a weak correlation between digital flexor tenosynovitis and SDFT injuries.

Injuries of the distal sesamoidean ligaments were diagnosed in 17 of 30 horses (57%). This finding agrees with the results of previous reports (Smith *et al.,* 2008, Sherlock *et al.,* 2009 and Gonzalez *et al.,* 2010). We diagnosed SSL desmitis more frequent than OSL desmitis. This could be attributed to the same alignment of SSL, SDFT and DDFT which receive the same strain during weight loading. This result agrees with results of Gonzalez *et al.* (2010) but differs from the results published by Sampson *et al.* (2007). Desmitis of SSL showed moderate correlations with other lesions, while OSL desmitis showed weak correlation however it was present with other lesions in all affected horses. This could be explained by the injury incidence of each ligament. Most of distal sesamoidean desmitis was recorded near the origin of these ligaments. This observation differs from several previous studies (Schneider *et al.,* 2003, Sampson et al., 2007, Smith *et al.,* 2008, Sherlock *et al.,* 2009 and Gonzalez *et al.,* 2010) that recorded it at ligament insertions. These controversial findings may be due to high susceptibility of distal sesamoidean ligaments to magic angle effect artifact of MRI (Smith and Dyson, 2011).

MRI was a helpful tool for 3D evaluation of adhesions between DDFT and proximal digital annular ligament and SSL. Moreover the extension and severity of adhesions could be assessed by MRI. Similarly, Elemmawy *et al.* (2019) measured adhesions between DDFT and SSL and discussed similar advantages of MRI in assessment of adhesions.

Cartilage erosions of pastern and/or fetlock were reported in 7 horses with several MRI abnormalities. Adhesions between proximal digital ligament (PDAL) and DDFT were moderately correlated with cartilage erosion (r=0.315). This may be due to spreading of the inflammatory process in the vicinity of pastern joint to the nearby tissues like DDFT and/or PDAL. In previous studies using MRI, cartilage lesions were underestimated (Dyson and Murray 2006, Werpy *et al.,* 2008 and Sherlock *et al.,* 2009). In the present study with low field MRI system, chronic osteoarthritis of pastern joint ranging from cartilage edema to osteophyte formation was imaged clearly by MRI and confirmed grossly. This may be due to high chronicity of the cases examined in our study. The authors suggested that accurate MRI sequences and slices selection are the most critical points for detection of cartilage erosions. T2 TIRM sequence taken by 0.3 T Magnetom C with TR 7780, TE 22, inversion time 90, number of averages (NEX) 2, magnetic field strength 0.3425, echo train length 7, slice thickness 3mm, slice spaces 3.3mm using Tx coil is the most helpful sequence for cartilage assessment.

Subchondral bone erosions or osseous cyst-like lesions were visible in 3 horses as focal signal hyperintensity representing the cystic fluid and surrounded by an area of signal hypointensity, presumably due to sclerosis and localized loss of bone architecture in all sequences. Similar findings were reported by Sherlock *et al.* (2009). Occasional obvious normal cyst of PI marrow at the level of thickest part of cortices was reported in a horse. Attention should be paid to differentiate this normal cyst from other clinically significant cystic lesions. This differentiation can be done by the anatomic location of the cyst.

The presence of small osteophytes was difficult to be imaged by MRI and couldn't be distinguished without guidance of radiographs. Similar findings were recorded by Gonzalez *et al.* (2010). Therefore, we recommend both radiography and MRI for a comprehensive evaluation of small osteophytes in fetlock and pastern regions.

In the present study, multiple MRI abnormalities were recorded in most horses. This usually was confusing to determine which primary lesion was. Here, the clinicians must interconnect clinical findings with the signal characteristics of the lesions in MR images hand in hand with information from other imaging modalities to identify the specific lesions integrated with the MRI results (Murray *et al.,* 2004 and Gonzalez *et al.,* 2010). This interconnection is a key factor for accurate diagnosis of the primary lesion.

Conclusions: Coexisting injuries of soft and osseous tissues of fetlock and pastern region are more common in draft horses. Investigation of all fetlock and pastern structures with appropriate selection of MRI sequences and interconnection of clinical findings and findings of other imaging modalities with MRI results s highly recommended for accurate diagnosis.

Authors contribution: All authors contributed in the article equally.

Acknowledgments: Many thanks should be paid to Dr. Emad Naoum, Brooke Charity Hospital Manager, Egypt for his assistance during this study.

REFERENCES

American association of equine practitioners, 2019. Definition and classification of lameness. Guide for veterinary service and judging of equestrian events. Lexington, KY. https://aaep.org/horsehealth/lameness -exams-evaluating-lame-horse. & Euthanesia guidelines, Published 1991. Accessed January, 2020.

Arensburg L, Wilderjans H, Simon O, *et al.,* 2011. Nonseptic tenosynovitis of the digital flexor tendon sheath caused by longitudinal tears in the digital flexor tendons: A retrospective study of 135 tenoscopic procedures. Equine Vet J, 43: 660-668.

Dyson SJ and Murray R, 2006. Osseous trauma in the fetlock region of mature sport horses. AAEP proceedings, 52: 443-446.

Dyson SJ and Murray R, 2007. Magnetic resonance imaging of the equine fetlock. Clin Tech Equine Pract, 6: 62–77.

Elemmawy YM, Senna NA, Abu-Seida AM, *et al.,* 2019. Suspensory Branch Desmitis in a horse: Ultrasonography, Computed Tomography. Magnetic Resonance Imaging and Gross Postmortem Findings. Equine Vet Sci, 80: 49-55.

Gibson KT, Burbidge HM and Anderson BH, 1997. Tendonitis of the branches of insertion of the superficial digital flexor tendon in horses, Aust Vet J, 75: 253.

Gonzalez LM, Schramme MC, Robertson ID, *et al.,* 2010. MRI features of metacarpo (tarso) phalangeal region lameness in 40 horses. Vet Radiol Ultrasound, 51: 404–414.

Hawkins JF, 2011. The draft horses, in: Baxter GM (editor), Adams and Stashak's lameness in horses. Wiley-Blackwell, West Sussex, UK, pp: 1655.

Johnston K and Nickels FA, 2011. The Standardbred racehorse, in: Baxter GM (editor), Adams and Stashak's lameness in horses. Wiley-Blackwell, West Sussex, UK, pp: 1593.

Knox PM and Watkins JP, 2006. Proximal interphalangeal joint arthrodesis using a combination plate-screw technique in 53 horses (1994–2003). Equine Vet J, 38: 538–542.

Martinelli MJ, Baker GJ, Clarkson RB, *et al.,* 1996. Magnetic resonance imaging of degenerative joint disease in a horse: a comparison to other diagnostic techniques. Equine Vet J, 28: 410–415.

Murray RC, Roberts BL, Schramme MC, *et al.,* 2004. Quantitative evaluation of equine deep digital flexor tendon morphology using magnetic resonance imaging. Vet Radiol Ultrasound, 45: 103–111.

Olive J, Mair TS and Charles B, 2009. Use of standing low-field magnetic resonance imaging to diagnose middle phalanx bone marrow lesions in horses. Equine Vet Edu, 21: 116-123.

Pool RR and Meagher DM, 1990. Pathological findings and pathogenesis of racetrack injuries. Vet Clin North Am-Equine Pract, 6: 1–30.

Sampson SN, Schneider RK, Tucker RL, *et al.,* 2007. Magnetic resonance imaging features of oblique and straight distal sesamoidean desmitis in 27 horses. Vet Radiol Ultrasound, 48: 303–311.

Schneider RK, Tucker RL, Habegger SR, *et al.,* 2003. Desmitis of the straight sesamoidean ligament in horses: 9 cases (1995–1997). J Am Vet Med Assoc, 222: 973–977.

Schramme MC and Smith RW, 2011. Diseases of the digital flexor tendon sheath, palmar annular ligament, and digital annular ligaments, in: Ross MW and SJ Dyson (editors): Diagnosis and management of lameness in the horse. WB Saunders, St. Louis, Missouri, US, 765–775.

Sherlock CE, Mair TS and Braake F, 2009. Osseous lesions in the metacarpo(tarso)phalangeal joint diagnosed using low-field magnetic resonance imaging in standing horses. Vet Radiol Ultrasound, 50: 13–20.

Smith M and Dyson S, 2011. Normal MRI anatomy, in: Murray RC (editor), Equine MRI. Wiley-Blackwell, UK, West Sussex, pp: 186.

Smith MW and Wright IM, 2006. Non-infected tenosynovitis of the digital flexor tendon sheath: a retrospective analysis of 76 cases. Equine Vet J, 38: 134-141.

Smith S, Dyson SJ and Murray RC, 2008. Magnetic resonance imaging of distal sesamoidean ligament injury. Vet Radiol Ultrasound, 49: 516-528.

Werpy NM, Ho CP, Pease A, *et al.,* 2008. Preliminary study on detection of osteochondral defects in the fetlock joint using low and high field strength resonance imaging. Proc 54th Am Assoc Equine Pract, 54: 447–451.